Many-objective design of tall buildings considering second order effects

Cláudio H. B. Resende [1], Afonso C. C. Lemonge[2], Luiz F. Martha[3]

[1]*Tecgraf Institute, PUC-Rio*
R. Marquês de São Vicente, 225, 22793-260, Gávea, Rio de Janeiro - RJ, Brazil
claudiohorta@tecgraf.puc-rio.br
[2]*Department of applied and computational mechanics - Federal University of Juiz de Fora*
Rua José Lourenço Kelmer s/n, 36036-900, Juiz de Fora - MG, Brazil
afonso.lemonge@ufjf.edu.br
[3]*Department of Civil and Environmental Engineering and Tecgraf Institute, PUC-Rio*
Rua Marquês de São Vicente, 225, 22451-900, Gávea, Rio de Janeiro - RJ, Brazil
lfm@tecgraf.puc-rio.br

Abstract. This research investigates the application of multi-objective optimization methodologies in developing economically viable and structurally efficient spatial steel constructions. It emphasizes the significance of optimizing performance alongside cost reduction in practical engineering scenarios. The investigation encompasses the minimization of maximum horizontal displacement, the maximization of the first natural frequency of vibration, the maximization of the critical load factor concerning the global buckling mode of the structure, and weight minimization as primary objectives. Furthermore, the analysis integrates considerations for both local and global second-order effects. Moreover, it delineates a systematic framework for selecting optimal designs, employing three distinct evolutionary algorithms grounded in differential evolution coupled with a multi-criteria decision-making approach.

Keywords: Multi-objective optimization; Steel structures; Differential evolution;

1 Introduction

Steel space frames are widely employed in civil engineering across various domains. Their applications span diverse structures, including large shopping centers, residential buildings, sports stadiums, museums, and cultural centers. Steel's superior strength-to-weight ratio makes it an attractive material for achieving lighter structural solutions. However, as steel frames increase in height, several critical challenges arise in design. These include horizontal displacements induced by wind loads, compromised dynamic behavior due to reduced natural vibration frequencies and increased flexibility, and diminished overall stability. The integration of bracing systems is crucial to mitigate these challenges arising from the inherent slenderness of such structures.

With advancements in engineering technology and rising population demands, the complexity of structural systems has increased concurrently. Simultaneously, the modern economic landscape has become highly competitive, necessitating the development of more efficient and economically viable projects. Structural optimization studies play a pivotal role in this context, aiming to determine optimal values for design variables that either minimize costs or maximize performance while meeting all project requirements.

Engineering design is a meticulous process involving critical decision-making from conceptualization to final detailing. Decision-making in engineering design is often intricate due to conflicting objectives. While solving a single-objective problem within an evolutionary framework is relatively straightforward, addressing multiple conflicting objectives results in a trade-off curve known as the Pareto front. Extracting optimal solutions from this front poses a significant challenge for decision-makers [1].

This study focuses on solving a multi-objective optimization problem related to a spatial steel frame, considering various types of bracing systems, orientation of the principal inertia axes of the columns, and approximate geometric nonlinear analysis. Meta-heuristic approaches, specifically differential evolution-based algorithms and a multi-criteria method for extracting solutions are employed. The remainder of this paper is structured as follows: Section 2 provides a brief overview of the materials and methods used; Section 3 outlines the formulation of the optimization problem; Section 4 details the numerical application conducted; and finally, Section 5 presents the

analysis of results, concluding remarks, and avenues for future research.

2 Materials and methods

Multi-objective optimization entails simultaneous consideration of conflicting objectives, yielding a set of non-dominated solutions and forming a Pareto front. According to the dominance principles articulated by Deb [2], a solution A dominates another solution B if it is either better or equal in all objective functions or strictly superior in at least one objective function. This study employs three differential evolution-based algorithms: Success History-based Adaptive Multi-Objective Differential Evolution (SHAMODE) by Panagant et al. [3], Success History-based Adaptive Multi-Objective Differential Evolution with Whale Optimization (SHAMODE-WO) enhanced by Mirjalili and Lewis [4], and Multi-Objective Meta-heuristic with Iterative Parameter Distribution Estimation (MMIPDE) proposed by Wansasueb et al. [5]. Dominance and crowding distance principles are applied to identify high-quality solutions, while constraint-based, non-dominated sorting ensures the ranking of feasible solutions. Furthermore, this study incorporates the Multi Tournament Decision Method (MTD) introduced by Parreiras and Vasconcelos [6], a predefined methodology used to extract solutions from the Pareto front and determine weighting coefficients based on the relative importance of each objective.

3 Formulation of the optimization problem

The goal of the multi-objective optimization problem is to obtain the Pareto trade-off curve with the optimal set of solutions, represented by the integer index vector $\mathbf{x} = I_1, I_2, ..., I_i$ (design variables) which defines the configuration of the bracing system, column orientations, and commercial steel profiles. This problem seeks to achieve four objectives: (i) minimizing the overall weight of the structure ($W(\mathbf{x})$), (ii) minimizing the maximum horizontal displacement ($\delta_{max}(\mathbf{x})$), (iii) maximizing the first natural frequency of vibration $f_1(\mathbf{x})$, and (iv) maximizing the critical load factor for global stability ($\lambda_{cr}(\mathbf{x})$). The formulation of this multi-objective problem is detailed in eq. (1), where $\mathbf{x}^L$ and $\mathbf{x}^U$ represent the lower and upper bounds of the design variables, respectively.

$$\begin{gathered} \min \quad W(\mathbf{x}) \quad \text{and} \quad \min \quad \delta_{max}(\mathbf{x}) \quad \text{and} \quad \max \quad f_1(\mathbf{x}) \quad \max \quad \lambda_{cr}(\mathbf{x}) \\ \text{s.t.} \quad \text{structural constraints} \\ \mathbf{x}^L \leq \mathbf{x} \leq \mathbf{x}^U \end{gathered} \tag{1}$$

The candidate vector of design variables is partitioned into five subsets identified by integer indexes, which specify configurations for the bracing system, orientations of column principal axis of inertia, and commercial steel profiles used for columns, beams, and bracer elements. The search space for these subsets includes 29 rolled profiles for columns and 56 for beams. Figure 1 provides a visual representation that links the design variables of the candidate vector.

The problem includes several constraints encompassing inter-story drift, Load and Resistance Factor Design (LRFD) interaction equations considering combined axial force and bending moments, LRFD shearing equations, and geometric constraints associated with beam-to-column and column-to-column connections. The maximum allowable inter-story drift is governed by $\bar{d} = h/500$, where h denotes the height between consecutive floors (eq. 2)). This constraint adheres to the guidelines specified in both the Brazilian code ABNT [7] and the American code ANSI [8].

$$\frac{d_{max}(\mathbf{x})}{\bar{d}} - 1 \leq 0 \tag{2}$$

The frame elements are required to satisfy the Load and Resistance Factor Design (LRFD) equations for combined flexural and bending effects:

$$\begin{cases} \dfrac{P_r}{P_c} + \dfrac{8}{9}\left(\dfrac{M_{rx}}{M_{cx}} + \dfrac{M_{ry}}{M_{cy}}\right) - 1 \leq 0 \quad if \quad \dfrac{P_r}{P_c} \geq 0.2 \\ \dfrac{P_r}{2P_c} + \left(\dfrac{M_{rx}}{M_{cx}} + \dfrac{M_{ry}}{M_{cy}}\right) - 1 \leq 0 \quad if \quad \dfrac{P_r}{P_c} < 0.2 \end{cases} \tag{3}$$

and the maximum allowable shearing equation:

$$\frac{V_r}{V_c} - 1 \leq 0 \tag{4}$$

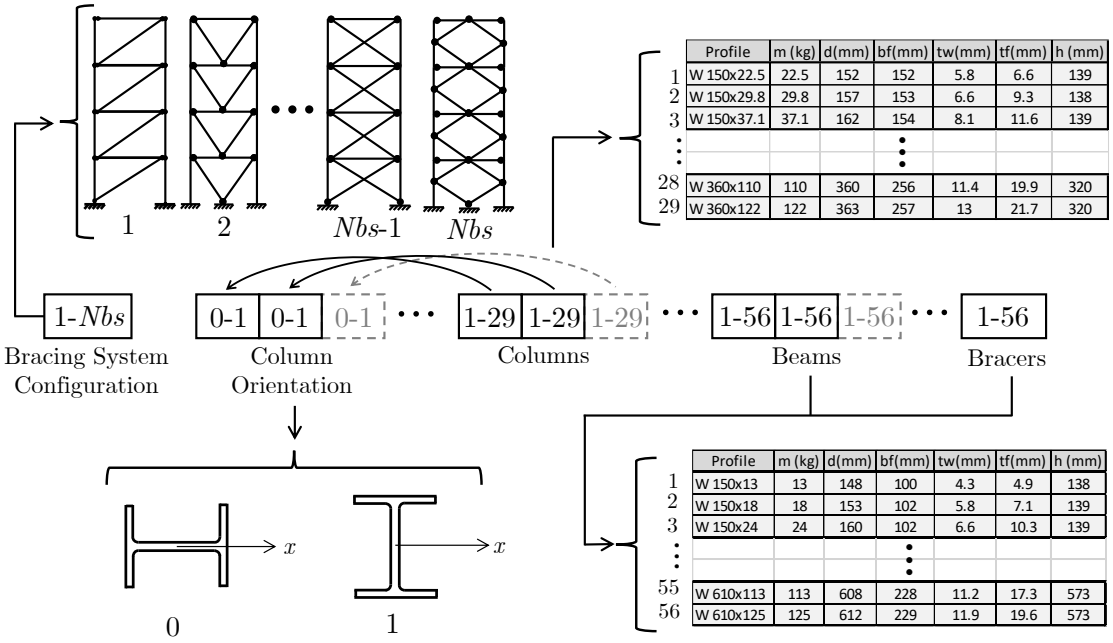

Figure 1. Candidate vector for a general problem, which includes the bracing system configuration, column orientation, and commercial profiles variables.

The required axial strength (P_r) and flexural strengths about the major (M_{rx}) and minor axes (M_{ry}) are compared with the available strengths of the members, denoted as P_c, M_{cx}, and M_{cy}, respectively. Furthermore, the allowable shearing strength equation considers the required shearing strength (V_r) and the available shearing strength (V_c).

The determination of the allowable strengths follows the approximate second-order analysis by amplifying the required strengths indicated by two first-order elastic analyses:

$$M_r = B_1 M_{nt} + B_2 M_{lt} \tag{5}$$

$$P_r = P_{nt} + B_2 P_{lt} \tag{6}$$

where:

- B_1 is the multiplier to account for $P-\delta$ effects;
- B_2 is the multiplier to account for $P-\Delta$ effects;
- M_{lt} is the first-order moment due to lateral translation of the structure only;
- M_{nt} is the first-order moment with the structure restrained against lateral translation;
- P_{lt} is the first-order axial force due to lateral translation of the structure only;
- P_{nt} is the first-order axial force with the structure restrained against lateral translation;
- M_r is the required second-order flexural strength;

This methodology is consistent with both the Brazilian code ABNT [7] and the American code ANSI [8].

The problem formulation integrates geometric constraints crucial for addressing structural considerations, particularly concerning connections between beams and columns, as well as between columns themselves. Constraints at beam-column connections prohibit attaching a beam with a flange wider than either the height of the column's web or its flange. Similarly, constraints at column-to-column connections ensure that profiles with greater depth or mass cannot be fitted over profiles with smaller dimensions. The geometric constraints are defined mathematically in equation (7). Here, h_{wi}, b_{fi}, and d_i represent the height of the web, the width of the flange, and the depth of the i-th member, respectively. Similarly, b_{fk} and b_{fj} denote the flange widths of the k-th and j-th members, while d_n indicates the depth of the n-th member. Additionally, m_i and m_n denote the linear mass of the i-th and n-th profiles, respectively. Finally, N_c signifies the total number of columns in the structure.

$$\frac{d_i}{d_n} - 1 \leq 0; \quad \frac{m_i}{m_n} - 1 \leq 0; \quad \frac{b_{fk}}{h_{wi}} - 1 \leq 0; \quad \frac{b_{fj}}{b_{fi}} - 1 \leq 0 \quad i = 1, N_c \tag{7}$$

4 Numerical application

The model to be optimized is depicted in Figure 2 and consists of a spatial frame with 16 floors and 16 bays, each with a height of 3.5 m. This model is inspired by a steel frame studied by Hasançebi [9]. Figure 2 also illustrates the available bracing configurations for the project.

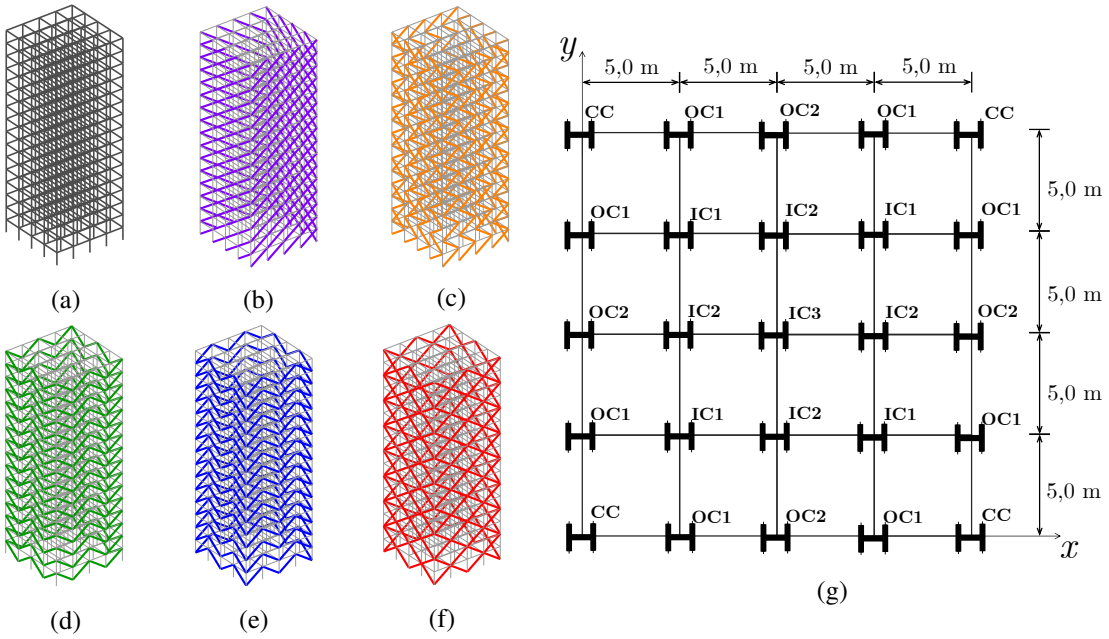

Figure 2. Spatial steel frame of 16 stories and 16 bays and its bracing system configurations. (a) 3D view; (b) "D"; (c) "Z"; (d) "V"; (e) "IV"; (f) "X"; (g) Plan view with columns' groups.

Wind loads are detailed in Table 1, and the gravitational loads acting on the beams are 7.85 kN/m for external beams and 22.21 kN/m for internal beams. The computational efforts required are determined using Equations (5) and (6).

Table 1. Nodal wind loads.

Story	Height (m)	C.N. (kN)	M.N.(kN)	Story	Height (m)	C.N. (kN)	M.N.(kN)
1	3,5	5,52	11,04	9	31,5	8,55	17,10
2	7,0	5,88	11,76	10	35,0	8,77	17,54
3	10,5	6,52	13,04	11	38,5	8,98	17,96
4	14,0	7,00	14,00	12	42,0	9,17	18,34
5	17,5	7,40	14,80	13	45,5	9,35	18,70
6	21,0	7,74	15,48	14	49,0	9,52	19,04
7	24,5	8,04	16,08	15	52,5	9,68	19,36
8	28,0	8,31	16,62	16	56,0	4,92	9,84

Six solutions are extracted using the Multi Tournament Decision (MTD) method, as described in the Materials and Methods section, with each extraction representing a specific scenario of weight combinations for the objective functions. These scenarios are as follows:

- Scenario 1: The weighting of $W(\mathbf{x})$ is $w_1 = 1.0$, of $\delta_{max}(\mathbf{x})$ is $w_2 = 0$, of $f_1(\mathbf{x})$ is $w_3 = 0$, and of $\lambda_{crt}(\mathbf{x})$ is $w_4 = 0$;
- Scenario 2: The weighting of $W(\mathbf{x})$ is $w_1 = 0$, of $\delta_{max}(\mathbf{x})$ is $w_2 = 1.0$, of $f_1(\mathbf{x})$ is $w_3 = 0$, and of $\lambda_{crt}(\mathbf{x})$ is $w_4 = 0$;
- Scenario 3: The weighting of $W(\mathbf{x})$ is $w_1 = 0$, of $\delta_{max}(\mathbf{x})$ is $w_2 = 0$, of $f_1(\mathbf{x})$ is $w_3 = 1.0$, and of $\lambda_{crt}(\mathbf{x})$ is $w_4 = 0$;
- Scenario 4: The weighting of $W(\mathbf{x})$ is $w_1 = 0$, of $\delta_{max}(\mathbf{x})$ is $w_2 = 0$, of $f_1(\mathbf{x})$ is $w_3 = 0$, and of $\lambda_{crt}(\mathbf{x})$ is $w_4 = 1.0$;
- Scenario 5: The weighting of $W(\mathbf{x})$ is $w_1 = 0.25$, of $\delta_{max}(\mathbf{x})$ is $w_2 = 0.25$, of $f_1(\mathbf{x})$ is $w_3 = 0.25$, and of $\lambda_{crt}(\mathbf{x})$ is $w_4 = 0.25$;

- Scenario 6: The weighting of $W(\mathbf{x})$ is $w_1 = 0.7$, of $\delta_{max}(\mathbf{x})$ is $w_2 = 0.1$, of $f_1(\mathbf{x})$ is $w_3 = 0.1$, and of $\lambda_{crt}(\mathbf{x})$ is $w_4 = 0.1$;

Five independent runs are performed for a population of 50 candidate vectors and 200 generations. This process is carried out for the SHAMODE, SHAMODE-WO, and MMIPDE algorithms. The Pareto front obtained with the six extracted scenarios highlighted is illustrated in Figure 3. The extracted solutions are detailed in Table 2 and depicted in Figure 4.

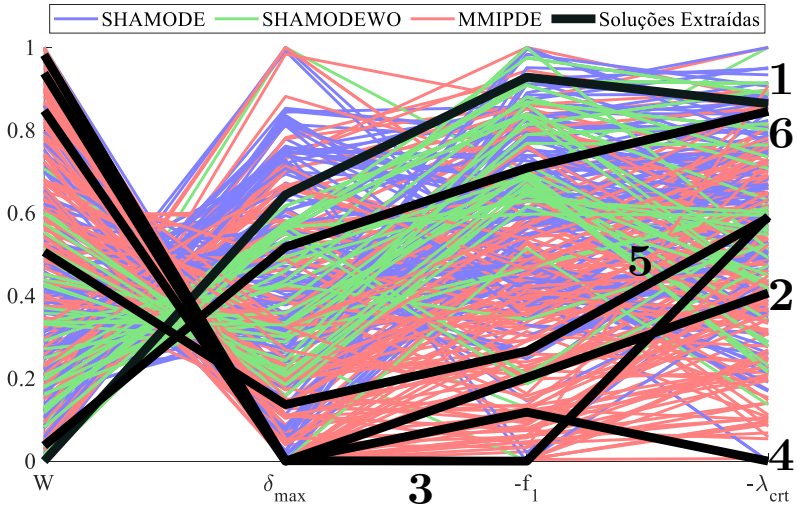

Figure 3. Pareto front and extracted solutions represented in normalized parallel coordinates.

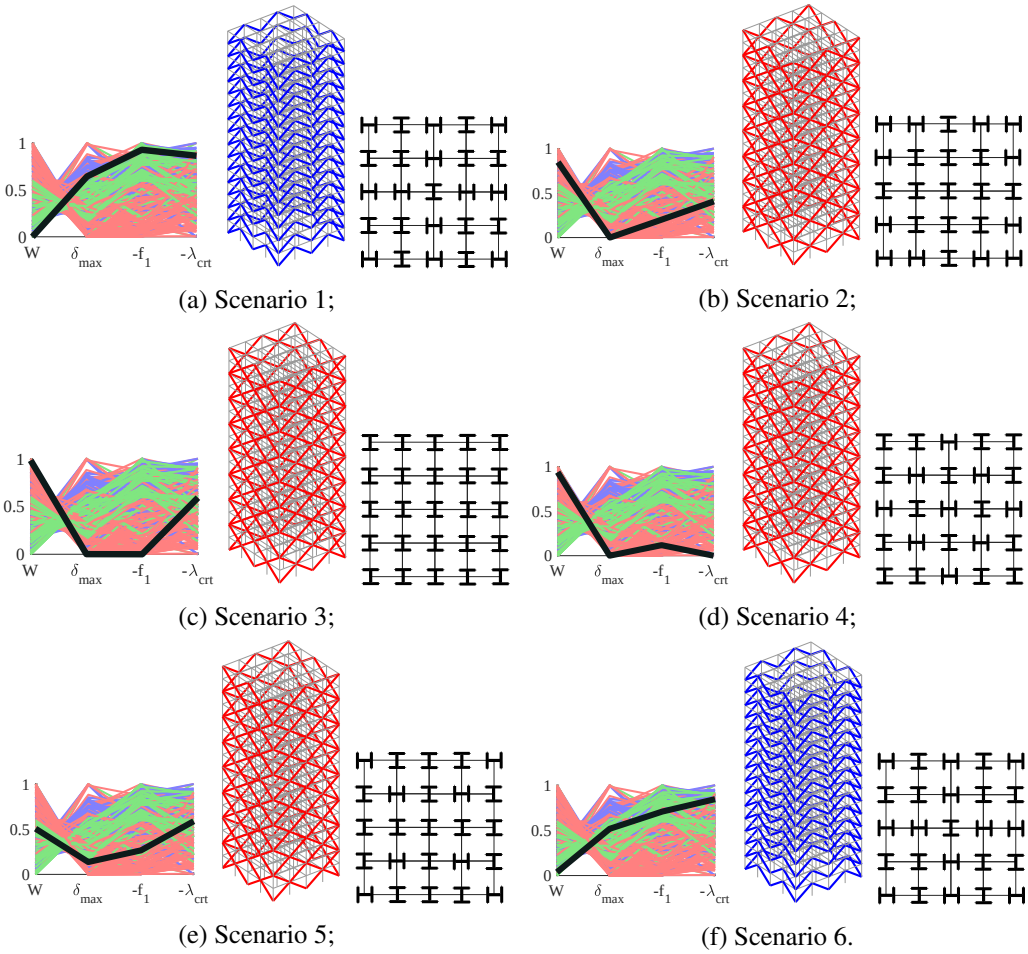

(a) Scenario 1; (b) Scenario 2;

(c) Scenario 3; (d) Scenario 4;

(e) Scenario 5; (f) Scenario 6.

Figure 4. Extracted solutions columns orientations and bracing systems.

Table 2. Detailed results for the extracted solutions from the Pareto front.

Scenario	1	2	3	4	5	6
Importance	[1 0 0 0]	[0 1 0 0]	[0 0 1 0]	[0 0 0 1]	[.25 .25 .25 .25]	[.7 .1 .1 .1]
Bracing System	**IV**	**X**	**X**	**X**	**X**	**IV**
Group (Stories)	W Profiles (Column Orientation)					
CC (1-4)	360x91	360X122	360X122	360X122	310x117	360x110
CC (5-8)	250x80	360X122	360X122	360X122	310x117	250x85
CC (9-12)	200x52	360X122	360X122	360X122	310x117	200x52
CC (13-16)	200x35.9	310x79	360X122	360X122	310x117	200x35.9
OC1 (1-4)	360x91	360X122	360X122	360X122	310x117	360x110
OC1 (5-8)	310x97	360X122	360X122	360X122	310x117	310x110
OC1 (9-12)	250x62	360X122	360X122	360X122	310x117	250x80
OC1 (13-16)	200x46.1	360X122	360X79	360X122	310x117	200x41.7
OC2 (1-4)	360x122	360X122	360x122	360x122	310x117	360x122
OC2 (5-8)	360x101	360X122	360X122	360X122	310x117	360x101
OC2 (9-12)	360x101	360X122	360X122	360X122	310x117	360x91
OC2 (13-16)	360x91	360X122	360X122	360X122	310x117	360x91
IC1 (1-4)	310x117	360X122	360x122	360X122	310x117	310x117
IC1 (5-8)	310x97	360X122	360X122	360X122	310x117	310x107
IC1 (9-12)	310x97	360X122	360X122	360X122	310x117	310x97
IC1 (13-16)	200x59	360X122	360X122	250x80	310x117	200x53
IC2 (1-4)	250x89	360X122	360X122	360x122	310x117	250x101
IC2 (5-8)	250x85	360X122	360X122	360X122	310x117	250x85
IC2 (9-12)	250x73	360X122	360X122	360X122	310x117	250x73
IC2 (13-16)	200x53	360X122	360X122	360X122	310x110	200x53
IC3 (1-4)	310x125	360X122	360X122	360x122	310x117	310x117
IC3 (5-8)	250x101	360X122	360X122	360X122	310x117	250x89
IC3 (9-12)	250x73	360X122	360X122	360X122	310x117	250x62
IC3 (13-16)	200x35.9	360X101	360X122	360X122	310x117	200x35.9
OB (1-4)	310x28.3	610x125	610X113	610X125	530x66	310x28.3
OB (5-8)	530x74	410x75	610X125	610X125	530x66	530x72
OB (9-12)	200x15	610x125	610X125	610X125	530x72	200x22.5
OB (13-16)	310x21	610x113	610X125	610X125	360x64	310x38.7
IB (1-4)	310x21	610x113	610X125	610X125	530x72	310x23.8
IB (5-8)	410x60	610x125	610X125	610X125	530x92	410x53
IB (9-12)	200x26.6	610x101	610X125	610X125	530x72	200x22.5
IB (13-16)	250x28.4	410x53	610X125	410x67	530x72	250x32.7
BC (1-16)	410x38.8	610x125	610X125	610X125	530x85	410x46.1
Objective Functions and Constraints						
$LRFD_{max}(\mathbf{x})$	0.99	0.62	0.63	0.69	0.68	0.85
$V_{max}(\mathbf{x})$	0.38	0.15	0.06	0.13	0.10	0.35
$d_{max}(\mathbf{x})$ (mm)	2.1	1.0	1.0	1.0	1.2	1.9
$\delta_{max}(\mathbf{x})$ (mm)	28.9	13.8	13.9	13.9	17.1	25.9
$f_1(\mathbf{x})$ (Hz)	0.46	1.13	1.32	1.21	1.07	0.66
$\lambda_{crt}(\mathbf{x})$	1.04	2.51	1.88	3.81	1.94	1.09
$W(\mathbf{x})$ (kg)	285022	695269	760631	739056	529834	303142
Algorithm	SHAMODE	MMIPDE	MMIPDE	MMIPDE	MMIPDE	SHAMODE

5 Conclusions

A crucial analysis in this numerical application involves observing the low critical load factors, which signify substantial stresses nearing global instability within the structure. This phenomenon predominantly stems from the considerable height of the building, resulting in substantial loads accumulating on the lower columns. Furthermore, incorporating second-order effects via stress amplification exacerbates stresses on structural components, thereby magnifying critical load factors.

In contexts involving buildings taller than those considered in this study, it becomes crucial to broaden the search space to include welded steel profiles, given the limitations associated with rolled profiles dimensions. Additionally, taller buildings often exhibit considerably lower vibration frequencies due to their higher flexibility and concentration of nodal masses at slab panel intersections, with observed values ranging between 0.46 Hz and 1.32 Hz. Adopting welded profiles and incorporating additional bracing subsystems, such as shear walls or rigid cores, emerge as viable strategies to mitigate these challenges.

Regarding the specified objectives, notable attention is directed toward solutions presented by the first four scenarios, each demonstrating superior performance in a primary objective at the expense of others. The lightest solution among the Pareto set (scenario 1) weighs $W(\mathbf{x}) = 285,022$ kg, associated with an "IV" shaped bracing system. Solutions corresponding to scenarios 2, 3, and 4 achieve optimal results in maximum displacement at the top $\delta(\mathbf{x}) = 13.8$ mm, vibration frequency $f_1(\mathbf{x}) = 1.32$ Hz, and critical load factor $\lambda_{crt}(\mathbf{x}) = 3.81$, respectively, all with an "X"-shaped bracing system.

Future research directions may involve exploring proposed optimization methodologies across various structural types and design variables and exploring alternative objective functions. Moreover, applying these techniques in real-world projects can offer insights into their effectiveness and applicability. Future efforts could also encompass advanced analysis methods such as iterative, incremental approaches, consideration of environmental and sustainable factors in structural optimization, and detailed examination of solutions derived through specialized software for steel structures. Additionally, integrating machine learning methods to minimize computational costs represents a promising avenue for future research.

Acknowledgements. The authors thank the Postgraduate Program in Civil and Environmental Engineering of PUC-Rio, Brazilian Agencies CNPq (grant 306186/2017-9 and 308105/2021-4) and CAPES for the financial support.

Authorship statement. The authors hereby confirm that they are the sole liable persons responsible for the authorship of this work, and that all material that has been herein included as part of the present paper is either the property (and authorship) of the authors, or has the permission of the owners to be included here.

References

[1] J. S. Arora. *Optimization of structural and mechanical systems*. World Scientific, Singapore, 2007.

[2] K. Deb. *Multi-objective Optimization using Evolutionary Algorithms*. John wiley & sons, Kanpur, 2001.

[3] N. Panagant, S. Bureerat, and K. Tai. A novel self-adaptive hybrid multi-objective meta-heuristic for reliability design of trusses with simultaneous topology, shape and sizing optimisation design variables. *Structural and Multidisciplinary Optimization*, vol. 60, n. 5, pp. 1937–1955, 2019.

[4] S. Mirjalili and A. Lewis. The whale optimization algorithm. *Advances in engineering software*, vol. 95, pp. 51–67, 2016.

[5] K. Wansasueb, N. Pholdee, N. Panagant, and S. Bureerat. Multiobjective meta-heuristic with iterative parameter distribution estimation for aeroelastic design of an aircraft wing. *Engineering with Computers*, vol. , pp. 1–19, 2020.

[6] R. Parreiras and J. Vasconcelos. Decision making in multiobjective optimization aided by the multicriteria tournament decision method. *Nonlinear Analysis: Theory, Methods & Applications*, vol. 71, n. 12, pp. e191–e198, 2009.

[7] ABNT. *NBR 8800: Projeto de estruturas de aço e de estruturas mistas de aço e concreto de edifícios.* ABNT Editora, Rio de Janeiro, Brasil, 2008.

[8] ANSI. *AISC 360-16 Specification for Structural Steel Buildings*. AISC, Chicago, USA, 2016.

[9] O. Hasançebi. Cost efficiency analyses of steel frameworks for economical design of multi-storey buildings. *Journal of constructional steel research*, vol. 128, pp. 380–396, 2017.